Int. J. Heat Mass Transfer. Vol. 30, No. 2, pp. 363–372, 1987
Printed in Great Britain

0017–9310/87 $3.00+0.00
Pergamon Journals Ltd.

Numerical computation of flow and heat transfer in finned and unfinned tube banks

M. FAGHRI and N. RAO*

Department of Mechanical Engineering, University of Rhode Island, Kingston, RI 02881, U.S.A.

(*Received* 1 *November* 1985 *and in final form* 5 *June* 1986)

Abstract—A finite volume numerical scheme is utilized to predict fluid flow and heat transfer characteristics in inline tube banks. The effect of equipping the tubes with longitudinal fins on the pressure drop and heat transfer is studied. The governing equations for fluid flow and heat transfer are numerically solved, with the assumption of periodic, fully developed flow. The numerical methodology utilizes the stepped boundary technique to approximate the tube surface. The tubes are maintained at a constant temperature, and the calculations are carried out for laminar flow and for a large range of Reynolds and Prandtl numbers. The results for the unfinned tube case are compared with previously published experimental data. The numerical results agree well with the experimental measurements. Representative results for the case of the finned tubes indicate, surprisingly, a decrease in the heat transfer rate, and small changes in the pressure drop, as a result of finning. The decrease in the heat transfer rate probably occurs because the fins are placed in the stagnation regions at the front and rear of the tubes, and thus do not increase the heat transfer.

INTRODUCTION

THERE have been a number of studies on the pressure drop and heat transfer characteristics of tube banks in cross flow. This field continues to attract researchers because of the importance of this configuration in the design of heat exchangers. Most of the earlier studies were experimental in nature, and an excellent review of such studies is given in Zukauskas [1]. In the recent past numerical methods have also been used to study the heat transfer and fluid flow in tube banks [2–5]. The complex geometry of the flow configuration poses an obstacle to the use of numerical methods. Different methods have been tried in order to surmount this obstacle, such as the conformal mapping technique of Thom and Apelt [2], and the hybrid polar–Cartesian grid approach of Launder and Massey [3], and Fujii and Fujii [4]. There have also been numerical computations using a Cartesian grid [5].

The objective of the present study is to extend the results of previous investigations by numerically computing the laminar flow and heat transfer characteristics of finned tube banks in cross flow. Apart from a recent experimental work by Sparrow and Kang [6], there does not seem to have been much research done on this problem. Sparrow and Kang [6] performed heat transfer and pressure drop experiments for the case of a staggered array tube banks equipped with longitudinal fins. They investigated geometrical parameters, including the placement of fins (at the front of the tube, at the rear, at the front and rear), the fin tip shape (blunt or contoured), and the fin thickness. The results were obtained for the transition/turbulent regime, with the Reynolds number, Re, (based on tube diameter, and the average velocity at the minimum cross-sectional area) ranging from 1000 to 8000. The results showed that a high degree of heat transfer enhancement can be obtained by finning.

The present contribution investigates the effect of finning on the fluid flow and heat transfer characteristics of an inline tube bank. In order to do so, the governing equations for momentum and energy conservation are numerically solved with the assumption of periodic, fully developed flow. The calculations are carried out for the low Reynolds number range ($1 < Re < 1000$). The heat transfer computations are carried out for four different values of Prandtl number ($Pr = 0.7, 5, 10, 20$). The mathematical formulation of the problem is presented in the next section.

MATHEMATICAL FORMULATION

A schematic view of the basic inline tube bundle, to be considered in this study, is shown in Fig. 1a. The solution domain, with the assumption of a periodic, fully developed flow, is confined to typical modules, or cells, shown in Fig. 1b. This study also considers the case of finned tube banks, in which the tubes are equipped with fins at the front and the rear. The solution domain for the case of finned tubes is shown in Fig. 2. In the case of the unfinned tube bundle, the geometry of the solution domain is specified by the tube diameter, D, the pitch, S_p, in the direction parallel to the flow, and the pitch, S_n, in the direction normal to the flow. When the tubes are equipped with fins, two additional parameters are required to be specified. These are the fin thickness,

* Present address: Department of Mechanical Engineering, University of Minnesota, Minneapolis, MN 55455, U.S.A.

NOMENCLATURE

A_w	heat transfer area
B	dimensionless pressure drop, $\beta D^3/\rho\nu^2$
C_p	specific heat
D	diameter of the tube
f	friction factor, $\Delta p/(2\rho\ V_m^2 N)$
g	inverse of dimensionless heat transfer area
G	ratio of outlet to inlet wall-to-bulk temperature
h	heat transfer coefficient
K	fluid thermal conductivity
L	length of fin
N	number of rows in tube bank
Nu	Nusselt number, hD/K
Nu_{av}	average value of Nusselt number
p	periodic component of dimensionless pressure
$\hat{p}$	periodic component of dimensional pressure
p^*	dimensional pressure
Δp	pressure drop across tube bank
Pr	Prandtl number, $\mu C_p/K$
Q	per cycle, wall heat transfer rate
Re	Reynolds number, $V_m D/\nu$
S_n	cylinder pitch in direction normal to flow
S_p	cylinder pitch in direction parallel to flow
t	fin thickness
T	temperature
T_w	wall temperature
T_b	bulk mean temperature
u^*, v^*	fluid velocity components
U, V	dimensionless fluid velocity components, defined in equation (1)
U_∞	free-stream velocity
V_m	average velocity at minimum cross-sectional area
x, y	space coordinates
X, Y	dimensionless space coordinates, defined in equation (1).

Greek symbols

β	pressure drop per unit length
θ	dimensionless temperature, $(T - T_w)/(T_b - T_w)$
λ	periodic function, defined in equation (9)
μ	dynamic viscosity
μ_b	viscosity at bulk temperature
μ_w	viscosity at wall temperature
ν	kinematic viscosity
ρ	density
σ	periodic quantity, defined in equation (8).

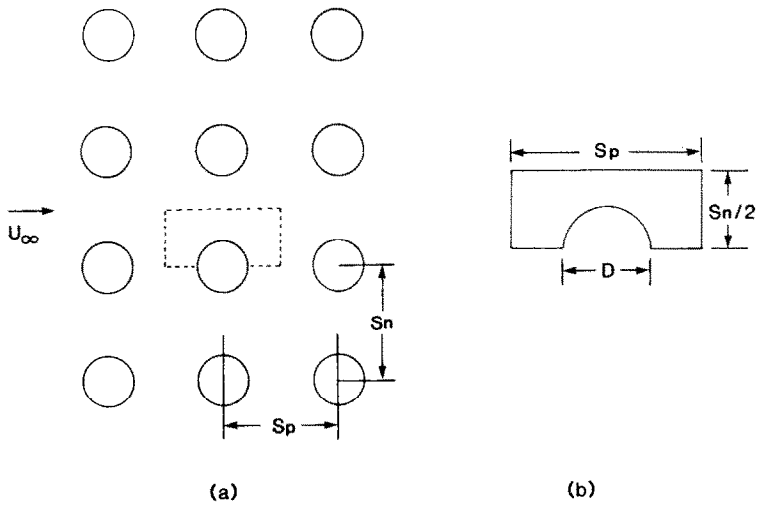

FIG. 1. (a) Inline tube bank. (b) Solution domain.

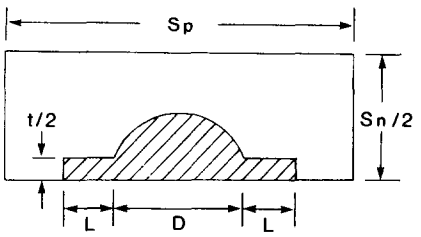

FIG. 2. Solution domain for finned tube bank.

t, and the fin length, L. The flow in the tube bundle is assumed to be steady, incompressible, fully developed and in the laminar flow regime.

Periodic, fully developed flow regime

The flow through an array of cylinders is analogous, in some respects, to the flow in a straight duct of constant cross-section. In both these flows, there is an entrance region beyond which the flow is fully developed. As in the case of ducts, if the entrance length is not too long, the flow characteristics of the array may be described by the fully developed flow alone. In a passage of periodically varying cross-section, the fully developed flow is characterized by a velocity field that repeats itself at corresponding axial stations in successive cycles. Furthermore, in such a regime, the pressures of cyclically corresponding locations decrease linearly in the downstream direction. Similarly, a periodic thermally developed regime exists for commonly encountered boundary conditions such as uniform wall temperature and uniform wall heat flux. The periodic, fully developed regime in this case is characterized by a cycle average heat transfer coefficient which is the same for each cycle of the periodic flow channel. The mathematical formulation for fully developed flow in flow passages of periodically varying cross-section has been developed in Patankar *et al.* [7], and is used here. Attention will now be turned to the conservation equations which describe the flow and heat transfer characteristics for an inline tube bank, with the assumption of a periodic, fully developed regime.

The conservation equations. The governing equations describing the flow are the continuity, momentum and energy equations. Laminar flow and constant thermophysical properties are assumed. The following dimensionless variables are used:

$$X = x/D, \quad Y = y/D, \quad U = u^*D/\nu, \quad V = v^*D/\nu \tag{1}$$

$$p = \hat{p}/\rho(\nu/D)^2, \quad B = \beta D^3/\rho\nu^2,$$
$$\theta = (T - T_w)/(T_b - T_w) \tag{2}$$

where u^*, v^* are the components of fluid velocity, and ρ and ν are the density and kinematic viscosity of the fluid, respectively. The bulk temperature, T_b, is defined as follows

$$T_b(x) = \left[\int_0^{S_n/2} TU\,dy\right]_x \Big/ \left[\int_0^{S_n/2} U\,dy\right]_x. \tag{3}$$

The pressure, p^* is expressed by $p^*(x,y) = -\beta x + \hat{p}(x,y)$, where β is a constant, and $\hat{p}(x,y)$ behaves in a periodic manner. The term βx represents the nonperiodic pressure drop that takes place in the flow direction. Thus, upon introduction of the dimensionless variables, the governing equations have the following forms

$$\partial U/\partial X + \partial V/\partial Y = 0 \tag{4}$$

$$U(\partial U/\partial X) + V(\partial U/\partial Y) = \partial^2 U/\partial X^2 + \partial^2 U/\partial Y^2 - \partial p/\partial X + B \tag{5}$$

$$U(\partial V/\partial X) + V(\partial V/\partial Y) = \partial^2 V/\partial X^2 + \partial^2 V/\partial Y^2 - \partial p/\partial Y \tag{6}$$

$$U(\partial\theta/\partial X) + V(\partial\theta/\partial Y) = (1/Pr)(\partial^2\theta/\partial X^2 + \partial^2\theta/\partial Y^2) + \sigma \tag{7}$$

with

$$\sigma = \left[\frac{2}{Pr}(\partial\theta/\partial X) - U\theta\right]\lambda + \frac{\theta}{Pr}[\lambda^2 + d\lambda/dX] \tag{8}$$

and

$$\lambda = [d(T_b - T_w)/dX]/(T_b - T_w) \tag{9}$$

where σ and λ are periodic quantities arising from the nature of the boundary conditions. Their values are determined as part of the solution process.

Note that the only parameters here are B, the dimensionless pressure drop, and Pr, the Prandtl number. The parameter B is related to Re, and is provided as an input for the computation. Note also that equations (5)–(7) retain the streamwise second derivatives $\partial^2 U/\partial X^2$, $\partial^2 V/\partial X^2$ and $\partial^2\theta/\partial X^2$ in recognition of the fact that large local values of these quantities may occur in the periodic fully developed flows.

To complete the discussion of the flow problem, it remains to discuss the boundary conditions. These are

$$U = V = \theta = 0 \tag{10}$$

on the cylinder and fin surface, and

$$\partial U/\partial Y = V = \partial\theta/\partial Y = 0 \tag{11}$$

on the symmetry boundaries. In addition, periodic boundary conditions are imposed on the inflow and outflow boundary segments. They take the form

$$U(Y)|_{X=S_p/D} = U(Y)|_{X=0} \tag{12}$$

$$V(Y)|_{X=S_p/D} = V(Y)|_{X=0} \tag{13}$$

$$\theta(Y)|_{X=S_p/D} = \theta(Y)|_{X=0}. \tag{14}$$

The parameters required as input for the computation are B, for the flow equations, and Pr for the

energy equation. A specification of the parameter B is equivalent to specifying the Reynolds number for the flow. In addition to these, the parameters describing the geometry, i.e. S_p/D, and S_n/D, t/D and L/D, are required as inputs prior to the computation.

In order to test the validity of the numerical methodology, calculations for the flow and heat transfer are carried out for a special case (case 1), for which experimental results exist. The computations for the pressure drop and heat transfer are carried out for an unfinned inline tube bank corresponding to model No. 2 in the experimental investigations of Bergelin *et al.* [8, 9]. The geometry parameters in this case have the following values

$$S_p/D = 1.25, \qquad S_n/D = 1.25. \tag{15}$$

The values of B are chosen so that the Reynolds number lies in the range $1 < Re < 1000$. The heat transfer calculations are performed for Prandtl numbers of 0.7, 5, 10 and 20.

Additional calculations are performed to study the effect of finning. Two sets of calculations are carried out, the first being for an inline array without fins (case 2), and the second for an inline tube bank equipped with fins (case 3). The geometry parameters for these calculations are

$$S_p/D = 2.4, \qquad S_n/D = 1.5, \qquad t/D = 0.2, \qquad L/D = 0.5. \tag{16}$$

The values of B are again chosen so that the Reynolds number of the flow lies in the range $1 < Re < 1000$. The heat transfer calculations are carried out for Prandtl numbers varying from 0.7 to 20.0.

Reynolds number, pressure drop, and Nusselt number

Attention will now be focused on the calculation of the Reynolds number, which is defined as follows

$$Re = V_m D/\nu \tag{17}$$

where V_m is the average velocity at the minimum cross-sectional area. For the inline tube bank the Reynolds number may be calculated as follows

$$Re = \frac{2}{[(S_n/D) - 1]} \int_0^{S_n/2D} U \, dY. \tag{18}$$

In much of the literature [3, 8, 9], the pressure drop is expressed in terms of the dimensionless friction factor, f, defined as

$$f = \Delta p/(2\rho V_m^2 N) \tag{19}$$

where Δp is the pressure across the tube bank, and N is the number of rows in the tube bank. For the flow geometry under consideration, the friction factor can be written in the form

$$f = 0.5B(S_p/D)/Re^2. \tag{20}$$

Finally, the cycle-average Nusselt number is obtained by

$$Nu = hD/k \tag{21}$$

where K is the fluid thermal conductivity, and h is the heat transfer coefficient, defined as

$$h = Q/A_w(\overline{T_w - T_b}) \tag{22}$$

where Q is the per cycle rate of heat transfer from the walls to the fluid, and A_w is the per-cycle heat transfer area, which is equal to $\pi D/2$ for the unfinned tube bank, and is equal to $(\pi D/2 + 2L)$ for the finned tube bank. The quantity $(\overline{T_w - T_b})$ is the average wall-to-bulk temperature difference. Both the log-mean and the arithmetic-mean temperature differences are used to evaluate $(\overline{T_w - T_b})$. Also, the effect of the inclusion of axial heat conduction in the per-cycle wall heat transfer Q is investigated. Four different expressions are derived for the calculation of the Nusselt number. $Nu(1)$ and $Nu(3)$ are obtained by assuming arithmetic-mean temperature difference, with and without inclusion of axial conduction in the heat transfer rate Q, respectively. $Nu(2)$ and $Nu(4)$ refer to the corresponding expressions obtained when the log-mean temperature difference is used. The four expressions used for the calculation of the Nusselt number are as follows:

$$Nu(1) = -g[(G - 1)/(G + 1)](S_n/D - 1)Re \cdot Pr \tag{23}$$

$$Nu(2) = g \ln(G)(S_n/D - 1)Re \cdot Pr/2 \tag{24}$$

$$Nu(3) = -g2[(G - 1)/(G + 1)] \times \left\{ Re \cdot Pr(S_n/D - 1)/2 - \int_0^{S_n/2D} \left(\lambda\theta + \frac{\partial\theta}{\partial X} \right)_{X=0} dY \right\} \tag{25}$$

$$Nu(4) = -g \ln(G)\{Re \cdot Pr(S_n/D - 1)/2 - \int_0^{S_n/2D} (\lambda\theta + \partial\theta/\partial X)_{X=0} \, dY \} \tag{26}$$

where G is the ratio of outlet to inlet wall-to-bulk temperature $(T_w - T_b)_{X=S_p/D}/(T_w - T_b)_{X=0}$, and g is the inverse of the dimensionless heat transfer area, which is equal to $2/\pi$ for the unfinned tube bank, and is equal to $[1/(\pi/2 + 2L/D)]$ for the finned tube bank. Interested readers may refer to ref. [10] for the derivation of the expressions for $Nu(1)$ and $Nu(3)$.

It should be noted that the boundary stepped method makes it difficult to obtain local heat transfer coefficients. In this paper, the heat transfer coefficients were obtained by calculating the influx of heat into, and the efflux out of, the solution domain. The difference between the two quantities yields the amount of heat transferred, Q, from the walls to the fluid.

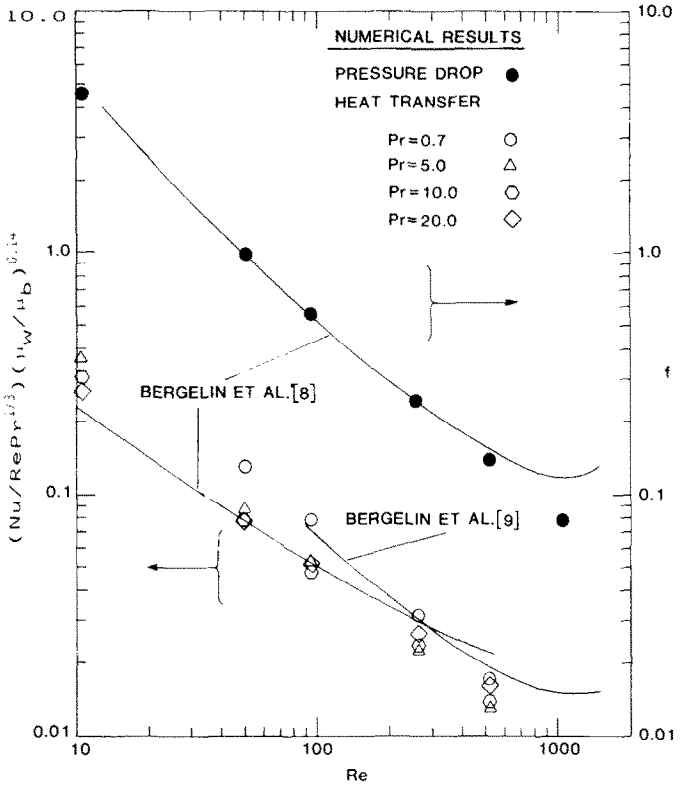

FIG. 3. Comparison of numerical results with experimental data of Bergelin *et al.* [8, 9].

Computational details

The governing flow equations, along with the boundary conditions, are solved using the finite-volume differencing methods developed in Patankar [11]. In this method, the flow equations are first discretized by integrating them over finite control volumes. The discretization procedure is based on the power-law scheme of Patankar [12]. The grid layout in this method uses staggered nodal locations for the velocity, while the pressure is computed at the main nodal locations. The discretized equations are solved by an iterative process. The pressure field is computed indirectly via the continuity equation, using the SIMPLER algorithm [11]. For the solution of the difference equations, a line-by-line method is used, which is a combination of cyclic tridiagonal matrix algorithm (TDMA) and Gauss–Siedel. The discretization procedure and solution methodology are tied in to the well-documented practices of Patankar [11]. Further details about the solution methodology may be obtained from Rao [13], wherein a system of convection–diffusion equations of a form similar to equations (4)–(7) have been numerically solved.

It should be noted that the presence of curved boundaries increases the complexity of the solution procedure. In this study, the cylinder surface is approximated by a series of steps, and the actual computation is carried out in Cartesian coordinates. A grid study showed that the solutions for the flow equations are reasonably grid independent, even for coarse computation grids. The solution for the energy equation is, however, very sensitive to the grid size used. It was thus decided to select the computation grid size on the basis of obtaining grid independent results for the energy equation alone. The grid dependence tests showed that, for the grid considered, and over the range $1 < Re < 1000$, the heat transfer results were accurate for a Prandtl number of 0.7. At higher Prandtl numbers, the accuracy of the results decreased at higher Reynolds numbers ($Re < 500$). This is because a very thin thermal boundary layer exists at higher values of ($Re \cdot Pr$), thus requiring more grid points to be placed close to the cylinder surface in order to obtain accurate results. In practice, the amount of processor time required for the calculations places restrictions on the maximum size of the computation grid that can be used.

The final computations were carried out for a grid containing 56 x 31 nodal points. About 300–500 iterations were necessary to obtain converged solutions for the velocity field, while the temperature field required only 75–150 iterations. The processing time required for the flow field computation ranged between 120 and 200 min, on a NAS7000 mainframe computer using an IBM OS/MVS operating system. The solution of the energy equation required 3–6 min of processor time. The results from the numerical computations are presented in the next section.

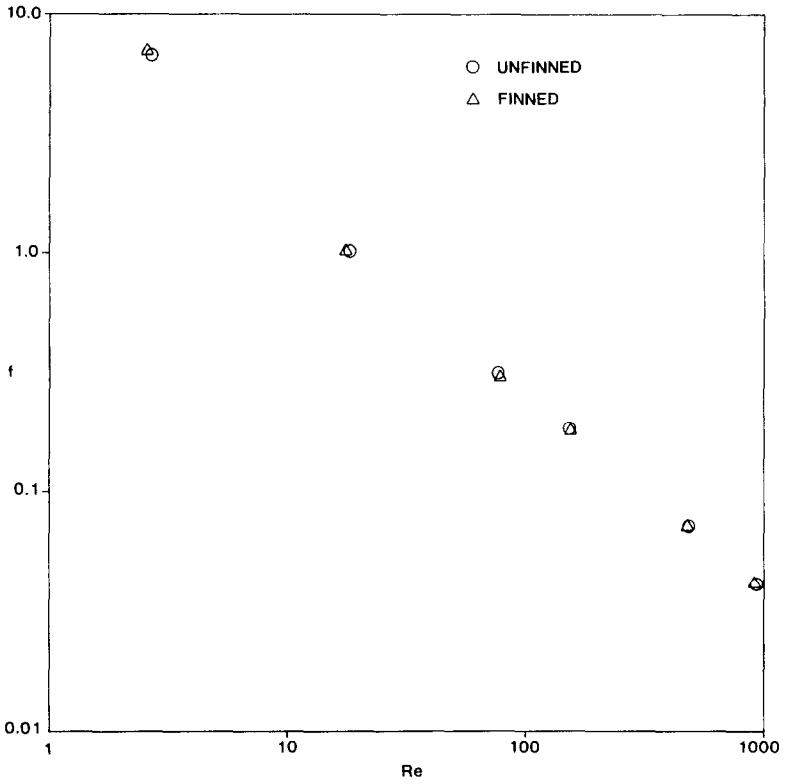

FIG. 4. Friction factor for finned and unfinned tube banks.

Table 1. Calculated values of friction factor and Nusselt number for the unfinned inline array tube bank

B	Re	f	Pr	$Nu(1)$	$Nu(2)$	$Nu(3)$	$Nu(4)$	Nu_{av}
40	2.7	6.584	20.0	5.348	5.531	5.341	5.524	5.436
280	18.23	1.011	5.0	5.586	5.657	5.566	5.636	5.611
			10.0	5.968	5.989	5.957	5.978	5.973
			20.0	6.730	6.737	6.724	6.732	6.731
1500	76.18	0.310	0.7	5.260	5.438	5.240	5.418	5.339
			5.0	6.929	6.937	6.923	6.931	6.930
			10.0	8.209	8.212	8.205	8.208	8.209
			20.0	10.79	10.79	10.79	10.79	10.79
3500	151.8	0.182	0.7	5.869	5.929	5.862	5.922	5.896
			5.0	8.173	8.176	8.171	8.174	8.174
			10.0	10.05	10.05	10.05	10.05	10.05
			20.0	13.69	13.69	13.69	13.69	13.69
14,000	486.8	0.071	0.7	7.077	7.087	7.075	7.085	7.081
			5.0	10.51	10.51	10.51	10.51	10.51
			10.0	13.64	13.64	13.64	13.64	13.64
			20.0	19.58	19.58	19.58	19.58	19.58
30,000	937.7	0.041	0.7	7.728	7.731	7.727	7.730	7.729
			5.0	11.86	11.87	11.86	11.87	11.87
			10.0	15.83	15.83	15.83	15.83	15.83
			20.0	23.29	23.29	23.29	23.29	23.29

RESULTS AND DISCUSSIONS

Representative results for the test case (case 1) shows good agreement with the experimental results of Bergelin *et al.* [8,9]. Figure 3 shows a plot of the friction factor, f, and the quantity $[(Nu/(Re\,Pr^{1/3})]$ vs the Reynolds number for the inline tube bank described by the geometry parameters in equation (15). Four different sets of data are plotted for the quantity $[(Nu/(RePr^{1/3})]$, corresponding to Prandtl numbers of 0.7, 5, 10 and 20. Also plotted are the experimental results of Bergelin *et al.* [8,9], who found that multiplying the quantity $[(Nu/RePr^{1/3})]$ by $(\mu_w/\mu_b)^{0.14}$ accounted for the effects of Prandtl

Table 2. Calculated values of friction factor and Nusselt number* for the finned inline array tube bank

B	Re	f	Pr	$Nu(1)$	$Nu(2)$	$Nu(3)$	$Nu(4)$	Nu_{av}
40	2.62	7.003	20.0	3.736	3.920	3.760	3.943	3.840
280	17.86	1.053	0.7	2.167	3.471	2.421	3.878	2.985
			5.0	3.887	3.953	3.887	3.953	3.920
			10.0	4.082	4.101	4.079	4.098	4.090
			20.0	4.479	4.485	4.477	4.483	4.481
1500	76.95	0.304	0.7	3.593	3.744	3.581	3.732	3.662
			5.0	4.396	4.401	4.389	4.394	4.395
			10.0	5.189	5.191	5.184	5.186	5.188
			20.0	6.910	6.910	6.910	6.910	6.910
3500	152.7	0.180	0.7	3.810	3.854	3.797	3.841	3.826
			5.0	5.083	5.085	5.080	5.082	5.082
			10.0	6.324	6.324	6.324	6.324	6.324
			20.0	8.768	8.768	8.768	8.768	8.768
14,000	485.7	0.071	0.7	4.430	4.436	4.428	4.435	4.432
			5.0	6.465	6.465	6.465	6.465	6.465
			10.0	8.334	8.334	8.334	8.334	8.334
			20.0	11.95	11.95	11.95	11.95	11.95
30,000	935.3	0.041	0.7	4.822	4.824	4.821	4.823	4.823
			5.0	7.234	7.234	7.234	7.234	7.234
			10.0	9.587	9.587	9.587	9.587	9.587
			20.0	14.11	14.11	14.11	14.11	14.11

* Based on actual area of heat transfer.

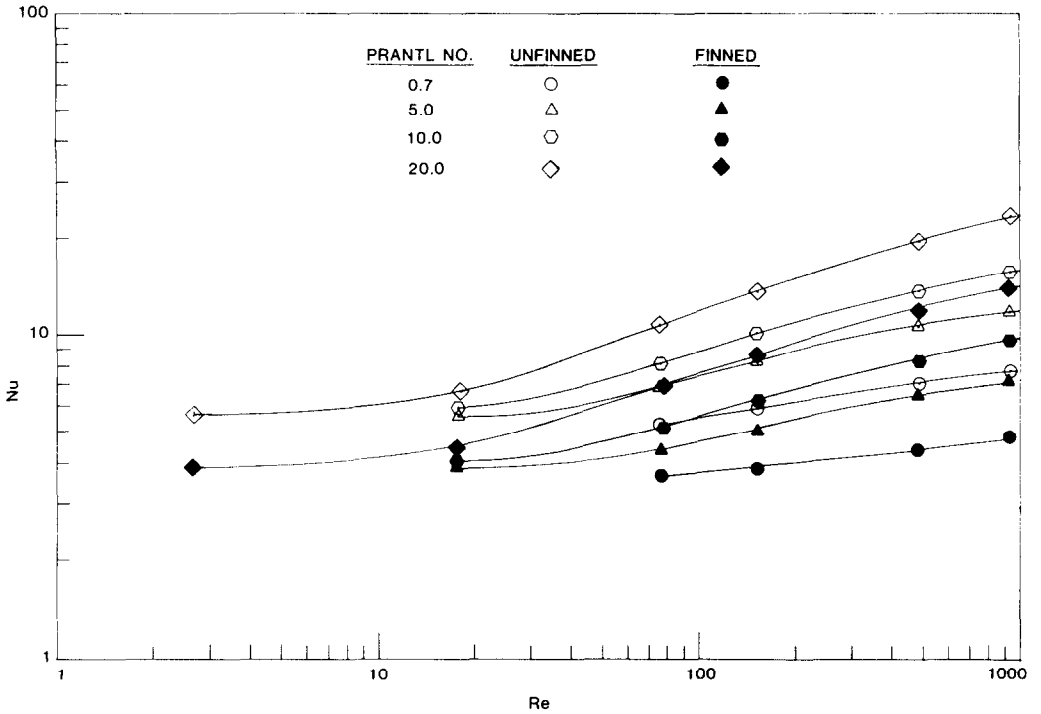

FIG. 5. Average Nusselt numbers for finned and unfinned tube banks.

number, and temperature dependence of viscosity, on their data. It is with this modified form that the comparison in Fig. 3 is made. As can be seen from the figure, the results for laminar flow agree very well for Re up to 1000. This is surprising since transition to turbulence is expected to occur at much lower values of Re. These results support the conclusion reached by Launder and Massey [3], who observed that for $Re < 1000$, "the effects of turbulence (or of some more ordered unsteadiness), if present, is not important".

It is reasonable to assume that the numerical methodology can yield reasonable results for the case of flow and heat transfer in finned tube banks. This is because the presence of fins would tend to act as 'flow straighteners' and would also damp out turbulence and vortex shedding. It is interesting to note from ref. [6] that the increase in heat transfer in

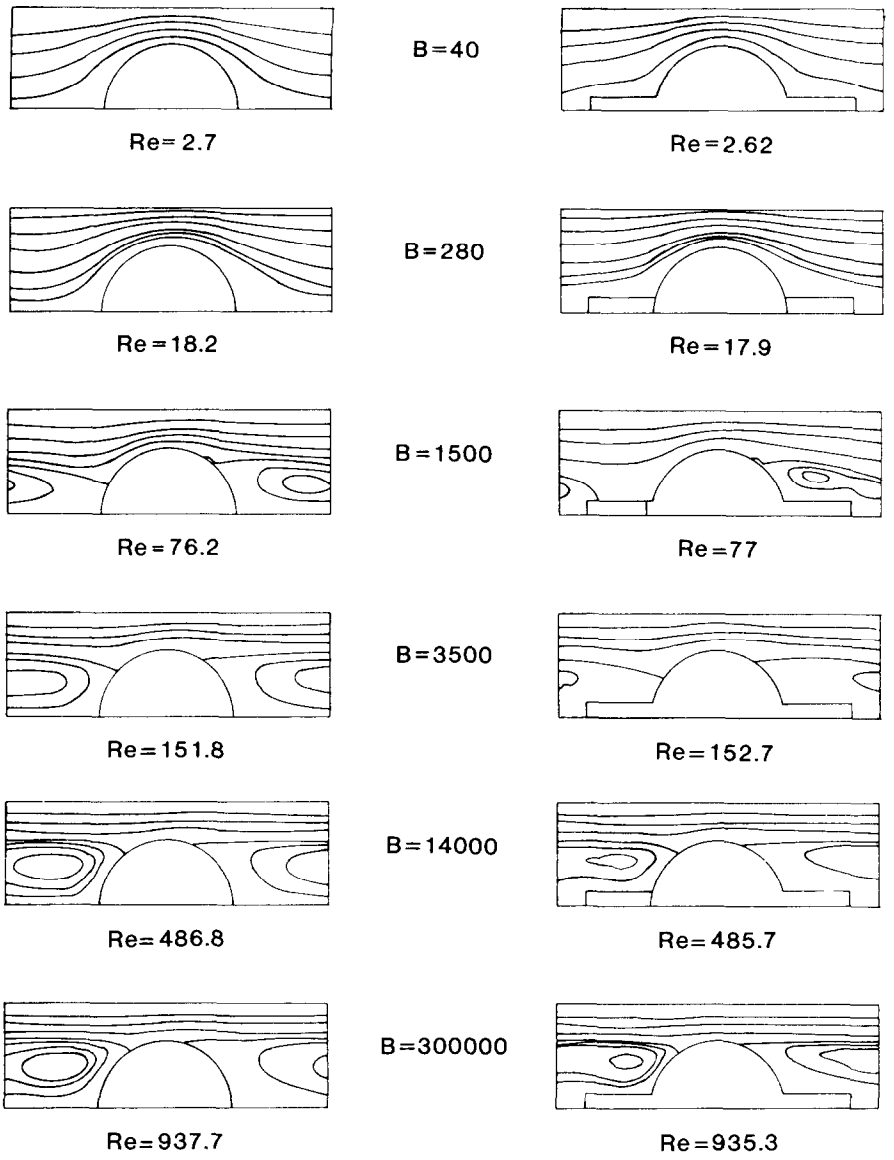

FIG. 6. Streamline plots for finned and unfinned tube banks.

finned tube banks is proportional to the increase in heat transfer area. It can be thus reasoned that finning, at least in staggered tube banks, does not lead to an increase in turbulence-related heat transfer.

The effect of finning, on the friction factor for the case of the inline tube bank with the geometry specified in equation (16), is seen in Fig. 4. This is a plot of the friction factor vs the Reynolds number, for the finned and unfinned tube banks. The calculated results are also listed in Tables 1 and 2, for the unfinned and finned case, respectively. Also tabulated are the Nusselt number results obtained from equations (22)–(25), for different values of Prandtl numbers. A comparison of the heat transfer rates for the finned and unfinned tube banks is graphically presented in Fig. 5. Here the average Nusselt number, Nu_{av} is plotted against the Reynolds number, for different values of Pr. The average Nusselt number is the arithmetic mean of $Nu(1)$, $Nu(2)$, $Nu(3)$ and $Nu(4)$. The closeness between the friction factor results for the finned and unfinned tube banks [see Fig. 4], suggest that the flow, in both cases, is similar. This is clearly seen in Fig. 6, which shows the streamline plots for the finned and unfinned cases at different values of the parameter B. It is seen that the fins are in the stagnation zones in the front and rear of each tube, and thus effect the flow in these regions only. The major part of the flow does not seem to feel the effect of the fins being present. The heat transfer results in Fig. 5 show that the Nusselt number decreases as a result of finning. This is probably again due to the fact that the fins are in the stagnation regions, and thus the increase in heat transfer area cannot be effectively used. Figure 7 shows a set of

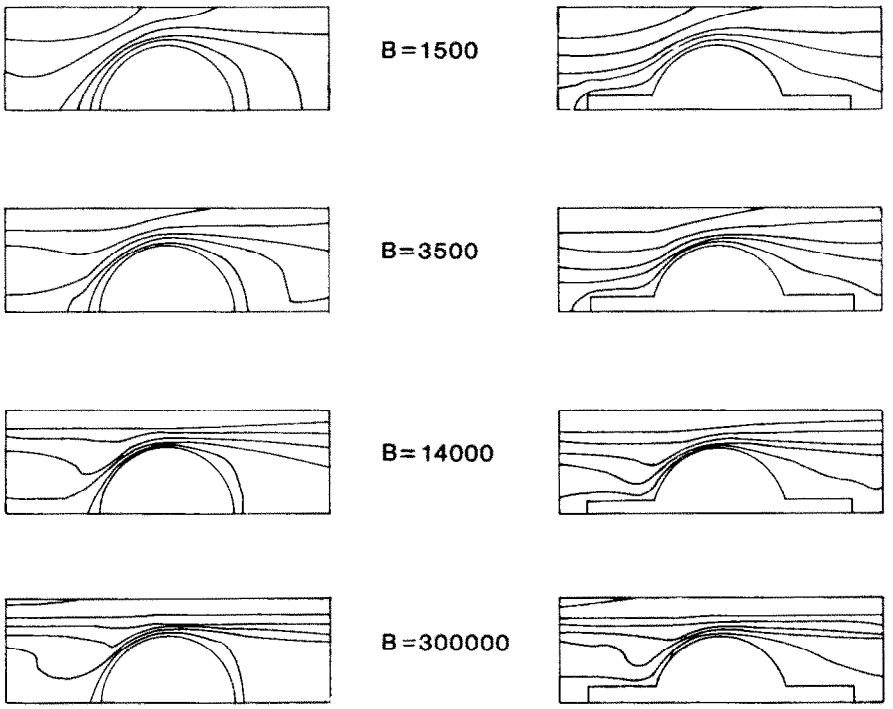

FIG. 7. Isotherm plots for finned and unfinned tube banks.

Table 3. Calculated values of Nusselt number* for the finned inline array tube bank

B	Re	Pr	$Nu(1)$	$Nu(2)$	$Nu(3)$	$Nu(4)$	Nu_{av}
40	2.62	20.0	6.115	6.415	6.153	6.454	6.284
280	17.86	0.7	3.547	5.682	3.962	6.347	4.885
		5.0	6.362	6.471	6.361	6.470	6.416
		10.0	6.681	6.712	6.676	6.707	6.694
		20.0	7.330	7.340	7.327	7.337	7.333
1500	76.95	0.7	5.880	6.128	5.861	6.108	5.994
		5.0	7.194	7.202	7.183	7.191	7.193
		10.0	8.492	8.495	8.485	8.488	8.490
		20.0	11.31	11.31	11.31	11.31	11.31
3500	152.7	0.7	6.236	6.307	6.215	6.286	6.261
		5.0	8.319	8.322	8.314	8.318	8.318
		10.0	10.35	10.35	10.35	10.35	10.35
		20.0	14.35	14.35	14.35	14.35	14.35
14,000	485.7	0.7	7.251	7.261	7.247	7.258	7.254
		5.0	10.58	10.58	10.58	10.58	10.58
		10.0	13.64	13.64	13.64	13.64	13.64
		20.0	19.56	19.56	19.56	19.56	19.56
30,000	935.3	0.7	7.892	7.895	7.890	7.894	7.893
		5.0	11.84	11.84	11.84	11.84	11.84
		10.0	15.69	15.69	15.69	15.69	15.69
		20.0	23.09	23.09	23.09	23.09	23.09

* Based on area of unfinned tube.

isotherm plots for the finned and unfinned tube banks for a Prandtl number of 0.7, and at different values of B. Again it is seen that the presence of the fins changes the temperature distribution only in the stagnation regions. Table 3 presents the calculated values of the Nusselt number for the finned tube bank, based on the heat transfer area of an unfinned tube bank. A comparison of Tables 1 and 3 shows that the heat transfer rate increases only for low values of Prandtl number ($Pr = 0.7$). At higher values of Pr there is very little change in the heat transfer rate.

In summary, it appears that longitudinal finning, in the case of inline tube banks, does not lead to any

significant increase in actual heat transfer. This is because the fins are in the midst of stagnation regions, and hence do not increase the heat transfer, despite the fact that they present a larger surface area over which heat transfer may occur. This is in contrast to the case of staggered tube banks [6], for which finning substantially increase the heat transfer.

REFERENCES

1. A. Zukauskas, Heat transfer from tubes in cross flow, *Adv. Heat Transfer* **8**, 93–160 (1972).
2. A. Thom and C. J. Apelt, *Field Computations in Engineering and Physics*. Van Nostrand, London (1961).
3. B. E. Launder and T. H. Massey, The numerical prediction of viscous flow and heat transfer in tube banks, *J. Heat Transfer* **100**, 565–571 (1978).
4. M. Fujii and T. Fujii, A numerical analysis of laminar flow and heat transfer of air in an inline tube bank, *Numer. Heat Transfer* **7**, 89–102 (1984).
5. R. F. Le Feuvre, Laminar and turbulent forced convection processes through in-line tube banks, Imperial College London, Mechanical Engineering Department, HTS/74/5 (1973).
6. E. M. Sparrow and S. S. Kang, Longitudinally-finned cross-flow tube banks and their heat transfer and pressure drop characteristics, *Int. J. Heat Mass Transfer* **28**, 339–350 (1984).
7. S. V. Patankar, C. H. Liu and E. M. Sparrow, Fully developed flow and heat transfer in ducts having streamwise-periodic variation of cross-sectional area, *J. Heat Transfer* **99**, 180–186 (1977).
8. O. P. Bergelin, G. A. Brown, H. L. Hull and F. W. Sullivan, Heat transfer and fluid friction during viscous flow across banks of tubes—III. A study of tube spacing and tube size, *Trans. Am. Soc. mech. Engrs* **72**, 881–888 (1950).
9. O. P. Bergelin, G. A. Brown and S. C. Doberstein, Heat transfer and fluid friction during flow across banks of tubes—IV. A study of the transition zone between viscous and turbulent flow, *Trans. Am. Soc. mech. Engrs* **74**, 953–960 (1952).
10. E. M. Sparrow and A. T. Prata, Numerical solutions for laminar flow and heat transfer in a periodically converging–diverging tube, with experimental confirmation, *Numer. Heat Transfer* **6**, 441–461 (1983).
11. S. V. Patankar, *Numerical Heat Transfer and Fluid Flow*. McGraw-Hill, New York (1980).
12. S. V. Patankar, A calculation procedure for two-dimensional elliptic situations, *Numer. Heat Transfer* **2** (1979).
13. N. Rao, Computer modelling of flow through fibrous filters. M.S. thesis, Department of Mechanical Engineering, University of Rhode Island, Kingston (1985).

CALCUL NUMERIQUE DE L'ECOULEMENT ET DU TRANSFERT THERMIQUE DANS DES RANGEES DE TUBES AILETES OU NON

Résumé—Un schéma numérique à volume fini est utilisé pour prédire les caractéristiques d'écoulement et de transfert thermique dans des bancs de tubes alignés. On étudie l'effet des ailettes longitudinales sur les tubes. Les équations du mouvement et du transfert de chaleur sont numériquement résolues, avec l'hypothèse d'un écoulement périodique pleinement développé. La méthodologie numérique utilise la technique de la frontière échelonnée pour approcher la surface du tube. Les tubes sont maintenus à température constante et les calculs sont effectués pour l'écoulement laminaire et pour un grand domaine de nombre de Reynolds et de Prandtl. Les résultats pour les tubes lisses sont comparés avec les données expérimentales publiées. Les résultats numériques s'accordent bien avec les mesures. Pour le cas des tubes ailetés, les résultats indiquent une diminution surprenante du transfert de chaleur et de faibles changements de la perte de charge résultant de l'ailetage. La décroissance du transfert de chaleur est probablement due au fait que les ailettes sont placées dans les régions d'arrêt devant et derrière les tubes et que ceci n'a pas l'effet d'augmenter le transfert.

NUMERISCHE BERECHNUNG VON STRÖMUNG UND WÄRMEÜBERGANG IN BERIPPTEN UND UNBERIPPTEN ROHRBÜNDELN

Zusammenfassung—Es wird ein numerisches Verfahren verwendet, um Strömung und Wärmeübergang in einem fluchtenden Rohrbündel zu berechnen. Der Einfluß einer Längsberippung auf den Druckabfall und den Wärmeübergang wird untersucht. Die maßgeblichen Gleichungen für Strömung und Wärmeübergang werden numerisch gelöst, wobei eine periodisch voll-entwickelte Strömung angenommen wird. Dabei wird das numerische Verfahren der gestuften Berandung angewandt, um die Rohroberfläche zu approximieren. Die Rohre werden auf konstanter Temperatur gehalten. Die Berechnungen erfolgen für laminare Strömung in einem weiten Bereich der Reynolds- und Prandtl-Zahl. Die Ergebnisse für unberippte Rohre werden mit jüngst veröffentlichten experimentellen Daten verglichen. Die numerischen Berechnungen stimmen gut mit diesen Daten überein. Repräsentative Ergebnisse für berippte Rohre zeigen überraschenderweise eine Verminderung des Wärmeüberganges und eine nur geringe Änderung des Druckabfalles als Folge der Berippung. Das Abfallen der Wärmeübergangs-Koeffizienten wird wahrscheinlich dadurch hervorgerufen, daß die Rippen im vorderen und hinteren Staubereich abgebracht waren, wodurch sich keine Erhöhung des Wärmeübergangs-Koeffizienten ergeben kann.

ЧИСЛЕННЫЙ РАСЧЕТ ТЕЧЕНИЯ И ТЕПЛООБМЕНА В ОРЕБРЕННЫХ И НЕОРЕБРЕННЫХ ПУЧКАХ ТРУБ

Аннотация—С помощью численной схемы конечного объема проведен расчет характеристик течения жидкости и теплопереноса в коридорных пучкак труб. Исследовано влияние продольного оребрения труб на перепад давления теплоперенос. Численно решены основные уравнения для потока жидкости и теплопереноса в допущении периодического, полностью развитого течения. При численном решении использовался метод ступенчатой границы для аппроксимации поверхности труб. Температура труб поддерживалась постоянной, и расчеты выполнялись для ламинарного режима течения в большом диапазоне значений чисел Рейнольдса и Прандтля. Проведено сравнение результатов расчетов для неоребренной трубы ранее опубликованными экспериментальными данными и отмечено их хорошее совпадение. Совершенно неожиданным результатом анализа данных, полученных для оребренных труб, оказалось снижение плотности теплового потока и небольшое изменение перепада давления за счет оребрения. Вероятно, уменьшение плотности теплового потока вызвано местоположением ребер в зонах торможения потока на передней и задней стенкак труб, в результате чего не происходит увеличения в интенсивности теплообмена.